

Retired A Stars and Their Companions II: Jovian planets orbiting κ Coronae Borealis and HD 167042 ¹

John Asher Johnson^{2,3}, Geoffrey W. Marcy³, Debra A. Fischer⁴, Jason T. Wright³, Sabine Reffert⁵, Julia M. Kregenow³, Peter K. G. Williams³, Kathryn M. G. Peek³

johnjohn@ifh.hawaii.edu

ABSTRACT

We report precise Doppler measurements of two stars, obtained at Lick Observatory as part of our search for planets orbiting intermediate-mass subgiants. Periodic variations in the radial velocities of both stars reveal the presence of substellar orbital companions. These two stars are notably massive with stellar masses of $1.80 M_{\odot}$ and $1.64 M_{\odot}$, respectively, indicating that they are former A-type dwarfs that have evolved off of the main sequence and are now K-type subgiants. The planet orbiting κ CrB has a minimum mass $M_P \sin i = 1.8 M_{\text{Jup}}$, eccentricity $e = 0.146$ and a 1208 day period, corresponding to a semimajor axis $a = 2.7$ AU. The planet around HD 167042 has a minimum mass $M_P \sin i = 1.7 M_{\text{Jup}}$ and a 412.6 day orbit, corresponding to a semimajor axis $a = 1.3$ AU. The eccentricity of HD 167042 b is consistent with circular ($e = 0.027 \pm 0.04$), adding to the rare class of known exoplanets in long-period, circular orbits similar to the Solar System gas giants. Like all of the planets previously discovered around evolved A stars, κ CrBb and HD 167042b orbit beyond 0.8 AU.

Subject headings: techniques: radial velocities—planetary systems: formation—stars: individual (κ CrB, HD 142091, HD 167042)

¹Based on observations obtained at the Lick Observatory, which is operated by the University of California.

²Department of Astronomy, University of California, Mail Code 3411, Berkeley, CA 94720

³Institute for Astronomy, University of Hawaii, Honolulu, HI 96822

⁴Department of Physics & Astronomy, San Francisco State University, San Francisco, CA 94132

⁵ZAH-Landessternwarte, Königstuhl 12, 69117 Heidelberg, Germany

1. Introduction

Most of what is known about planets outside of our Solar System comes from Doppler surveys of Sun-like stars, with spectral types ranging from K0V to F8V and masses between 0.8 and 1.2 M_{\odot} (Valenti & Fischer 2005; Butler et al. 2006b; Takeda et al. 2007). However, recent results from planet searches around low-mass M dwarfs (Bonfils et al. 2005; Endl et al. 2006; Butler et al. 2006a) and evolved, intermediate-mass stars (Reffert et al. 2006; Johnson et al. 2006a; Sato et al. 2007; Niedzielski et al. 2007; Lovis & Mayor 2007) have expanded into the frontiers at either end of the stellar mass range. These surveys have begun to reveal important relationships between stellar mass and the properties of exoplanets. For example, planets around “retired” (evolved) A-type stars reside preferentially in wide orbits, with semimajor axes $a \gtrsim 0.8$ AU (Johnson et al. 2007b) and appear to have larger minimum masses than planets around Sun-like stars (Lovis & Mayor 2007). Also, the occurrence rate of Jovian planets ($M_P \sin i \geq 0.5 M_{\text{Jup}}$, $a \leq 2.5$ AU) increases with stellar mass, rising from $< 2\%$ around M dwarfs, to approximately 9% around F and A stars (Johnson et al. 2007a).

The effects of stellar mass on other characteristics of exoplanets, such as orbital eccentricity and multiplicity, will become evident as the sample of planets around intermediate-mass stars grows. Here, we report the detection of two Jovian planets orbiting stars with masses of 1.64 M_{\odot} and 1.80 M_{\odot} . These planet detections come from our sample of intermediate-mass subgiants that we have been monitoring at Lick and Keck Observatories (Johnson et al. 2006a). We describe our observations in § 2. In § 3 we present our data, and describe the characteristics of the host stars and the orbits of their planets. We conclude in § 4 with a summary of our results and a discussion of the properties of planets orbiting evolved A-type stars.

2. Observations and Doppler Measurements

We have been monitoring a sample of 159 evolved stars at Lick and Keck Observatories for the past 3.5 years. The stars were selected from the *Hipparcos* catalog based on the color and magnitude criteria described by Johnson et al. (2006a), namely $0.5 < M_V < 3.5$, $0.55 < B-V < 1.0$, and $V \lesssim 7.6$. We exclude from our sample clump giants with $B-V > 0.8$ and $M_V < 2.0$, as well as stars within 1 mag of the mean *Hipparcos* main sequence, as defined by (Wright 2005). These criteria allow us to take advantage of the widely spaced, nearly parallel stellar model tracks of the subgiant branch to estimate precise ages and masses.

We obtained Doppler measurements of the stars presented here using the 3 m Shane

and 0.6 m Coude Auxiliary Telescope (CAT) at Lick Observatory. Both telescopes feed the Hamilton spectrometer (Vogt 1987), which has a resolution of $R \approx 50,000$ at $\lambda = 5500 \text{ \AA}$. Doppler shifts are measured from each spectrum using the iodine cell method described in detail by Butler et al. (1996) and summarized as follows. A temperature-controlled Pyrex cell containing gaseous iodine is placed at the entrance slit of the spectrometer. The dense set of narrow molecular lines imprinted on each stellar spectrum from 5000 to 6000 \AA provides a robust wavelength scale for each observation, as well as information about the shape of the spectrometer’s instrumental response (Marcy & Butler 1992).

Traditionally, the Doppler shift of each stellar spectrum is measured with respect to an observed, iodine-free template spectrum. These template observations require higher signal and resolution than normal radial velocity observations, which in turn necessitates longer exposure times. Given our large target list and the small aperture of the CAT, obtaining a traditional template for each star would represent a significant fraction of our allocated observing time, resulting in a smaller than optimal target list. We therefore perform a preliminary analysis of each star’s observations using a synthetic, “morphed” template spectrum following the method described by Johnson et al. (2006b). Stars showing conspicuous Doppler variations are reanalyzed using a traditional template to verify the signal and search for a full orbital solution.

Internal uncertainties for each velocity measurement are estimated from the standard deviation of the mean velocity measured from the ~ 700 segments analyzed in each echelle spectrum. A typical $V = 6$, K0 star requires a 3600 second exposure on the CAT for a signal-to-noise ratio (S/N) of 180 pix^{-1} , which produces an internal precision of 3–4 m s^{-1} . The same star observed on the Shane requires 300 seconds for the same S/N owing to differences in the the collecting area and plate scale at the spectrometer entrance slit. The radial velocities for the two stars presented here are listed in Table 1 and Table 2.

3. Stellar Properties and Orbital Solutions

Our methods for determining the properties of our target stars are described in Johnson et al. (2007b) and summarized briefly as follows. We use the LTE spectral synthesis code SME (Valenti & Fischer 2005) to estimate stellar effective temperatures, surface gravities, metallicities, and projected rotational velocities by fitting a synthetic spectrum to each star’s iodine-free template spectrum. We use the Stephan-Boltzmann Law to relate each star’s radius and luminosity to its effective temperature, parallax-based distance and bolometric correction. To estimate stellar masses and ages, we interpolate each star’s *Hipparcos* absolute magnitude, $B - V$ color and SME-derived metallicity onto the stellar interior model grids

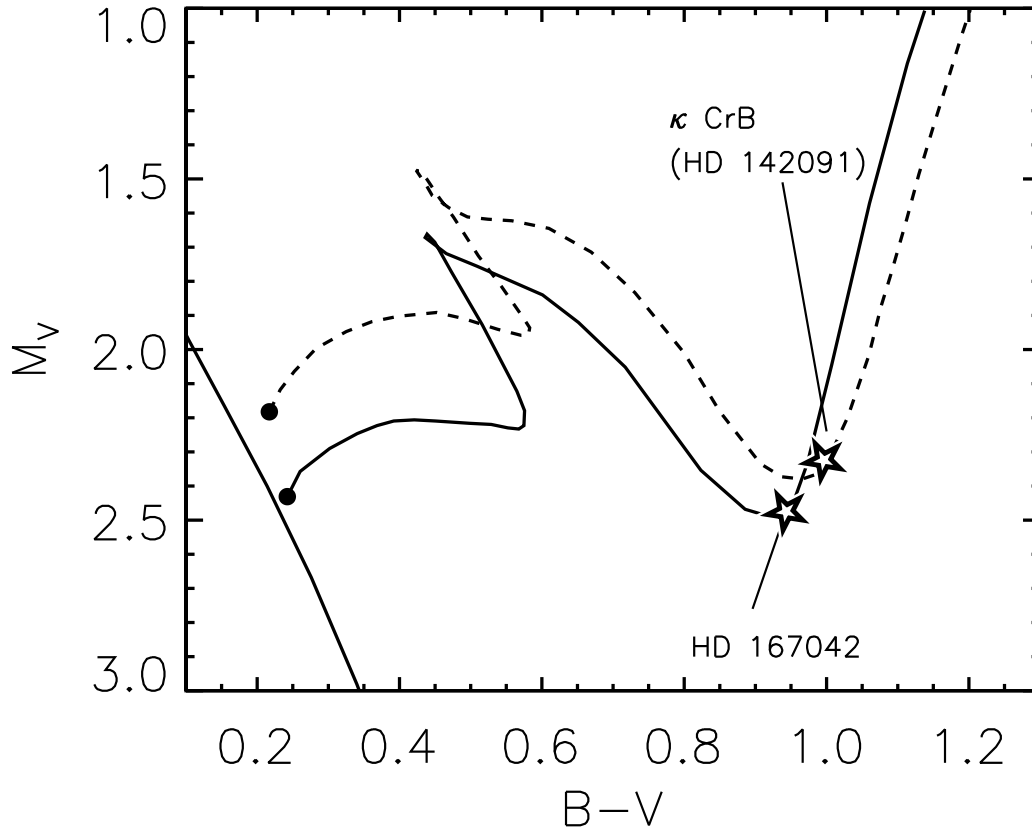


Fig. 1.— H-R diagram illustrating the properties of the two subgiant planet host stars (pentagrams) compared to their main-sequence progenitors (filled circles). The connecting lines represent the Girardi et al. (2002) theoretical mass tracks interpolated for each star’s metallicity. The thick, diagonal line is the zero-age main sequence assuming $[\text{Fe}/\text{H}]=0.0$.

computed by Girardi et al. (2002). The stellar properties and uncertainties are summarized in Table 3. The position of the two stars in the H-R diagram is shown in Figure 1, along with their theoretical mass tracks and zero-age main sequence.

Johnson et al. (2007b) estimate uncertainties of 7% in stellar mass and 1 Gyr for ages. Uncertainties in the SME-derived parameters are given by Valenti & Fischer (2005), however these estimates are based primarily on a sample of main-sequence stars and may be unrepresentative of the values obtained for our subgiants. We therefore estimate uncertainties in the spectroscopic parameters by exploring the degeneracy of the best-fit solution using different input guesses to the SME code. We first solve for the best-fit solution, and then use the

resulting parameters as input for two additional solutions, with ± 100 K perturbations on T_{eff} . The standard deviations of the parameters from the three SME trials are then adopted as the 1σ parameter uncertainties. In cases when our error estimates are less than those of Valenti & Fischer (2005), we adopt the latter values.

We search for the best fitting Keplerian orbital solution to each radial velocity time series using a Levenberg–Marquardt, least–squares minimization, and we estimate the uncertainties in the orbital parameters using a bootstrap Monte Carlo method. We first subtract the best–fit Keplerian from the measured velocities. The residuals are then scrambled and added back to the original measurements, and a new set of orbital parameters is obtained. This process is repeated for 1000 trials and the standard deviations of the parameters from all trials are adopted as the formal 1σ uncertainties.

In the following subsections we describe the properties of the two new host stars and planet candidates discovered from our sample of subgiants.

3.1. κ CrB

κ Coronae Borealis (κ CrB, HD 142091, HR 5901, HIP 77655) is listed in the SIMBAD database¹ with a spectral type K0IV and in the *Hipparcos* catalog as a K0III–IV star with $V = 4.79$ and $B - V = 0.996$, and a parallax–based distance of 31.1 pc (ESA 1997). The star’s apparent magnitude and distance yield an absolute magnitude $M_V = 2.32$, placing the star 4.3 mag above the mean main sequence of stars in the Solar neighborhood (Wright 2005). The color and absolute magnitude of κ CrB suggest an evolved star on the subgiant branch near the base of the red giant branch, in agreement with its published spectral classifications.

Our LTE spectral analysis suggests that κ CrB is metal–rich, with $[Fe/H] = +0.14 \pm 0.05$. Our spectral analysis also yields $T_{eff} = 4960 \pm 70$ K, $V_{rot} \sin i = 3.0 \pm 0.5$ km s^{−1} and surface gravity, $\log g = 3.45 \pm 0.09$. We estimate the mass and age of κ CrB by interpolating the star’s color, absolute magnitude and metallicity onto the Girardi et al. (2002) stellar interior models. We find a stellar mass $M_* = 1.80 M_\odot$ and an age of 2.5 Gyr. We also estimate a luminosity $L_* = 12.3 L_\odot$ and radius $R_* = 4.71 R_\odot$, assuming a bolometric correction -0.302 . The properties of κ CrB are summarized in Table 3.

To assess the photospheric stability of κ CrB, we searched the *Hipparcos* Epoch Pho-

¹<http://cdsweb.u-strasbg.fr/>

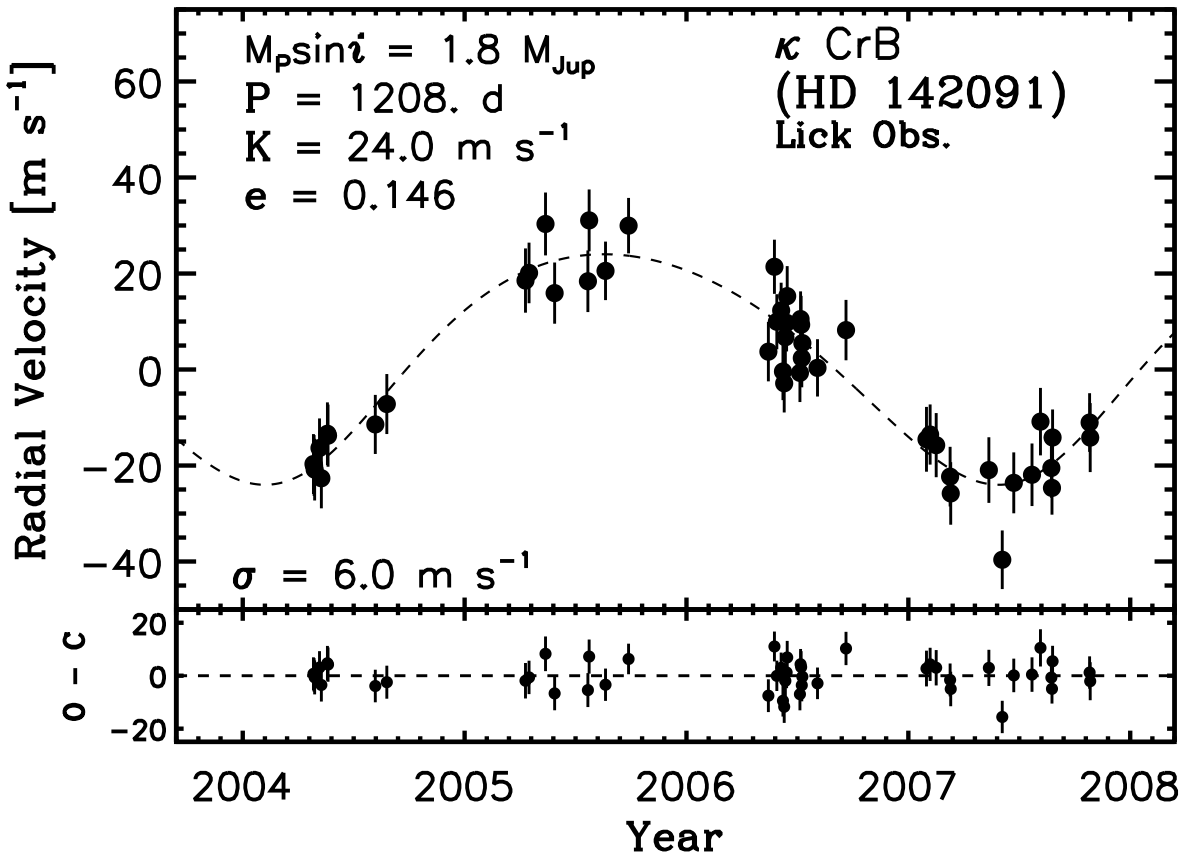


Fig. 2.— Radial velocity time series for κ CrB (HD 142091) measured at Lick Observatory. The dashed line shows the best-fit orbital solution, which has an orbital period of 3.309 years and $\sqrt{\chi^2_\nu} = 0.97$.

tometry database² and found 135 observations. The measurements have a mean uncertainty of 4.7 mmag and have an rms scatter of 4.7 mmag over a time span of 3.1 years³. Given its photometric stability, we can rule out significant pulsation modes that can contribute to intrinsic radial velocity variability. Further, based on the lack of emission in its CaII H&K line core, we measure $\log R'_{HK} = -5.40$ indicating κ CrB is chromospherically inactive, similar to other evolved stars (Wright et al. 2004).

Beginning in 2004 April, we collected 48 Doppler measurements at Lick Observatory, which are listed in Table 1 together with their date of observation and internal uncertainties.

²<http://www.rssd.esa.int/index.php?project=HIPPARCOS>

³After rejecting a single outlier

The velocities are also shown in Figure 2, and the error bars represent the quadrature sum of the internal measurement uncertainties and 5 m s^{-1} of jitter, which is typical for the intrinsic Doppler variability of subgiants similar to $\kappa \text{ CrB}$ (Johnson et al. 2007b).

Also shown in Figure 2 is the best fitting Keplerian orbital solution with a period $P = 1208 \pm 30$ days, eccentricity $e = 0.146 \pm 0.08$ and velocity semiamplitude $K = 24.0 \pm 1 \text{ m s}^{-1}$. The rms scatter of the data about the fit is 6.0 m s^{-1} and the reduced $\sqrt{\chi^2_\nu} = 0.97$. Based on our stellar mass estimate of $M_* = 1.80 M_\odot$, the orbital solution gives a minimum planet mass $M_P \sin i = 1.8 M_{\text{Jup}}$ and semimajor axis $a = 2.7 \text{ AU}$. The orbital parameters of $\kappa \text{ CrB}$ are summarized in Table 4.

3.2. HD 167042

HD 167042 (HR 6817, HIP 89047) is listed in the SIMBAD database with a spectral type K1 III, suggesting the star is on the giant branch. The *Hipparcos* catalog gives $V = 5.97$, $B - V = 0.943$, and a parallax-based distance of 50.0 pc (ESA 1997). Given its distance and apparent magnitude, we calculate an absolute magnitude $M_V = 2.48$, which places it 4.2 mag above the average main sequence of stars in the Solar neighborhood (Wright 2005). The position of HD 167042 in the H–R diagram indicates the star is better classified as a K1 IV subgiant near the upturn to the red giant branch, rather than a luminosity class III giant.

Based on our LTE spectral analysis (SME; Valenti & Fischer 2005), we find that HD 167042 has Solar metal abundance with $[\text{Fe}/\text{H}] = +0.05 \pm 0.06$, and is slowly rotating with $V_{\text{rot}} \sin i = 2.5 \pm 0.5 \text{ km s}^{-1}$. Our spectroscopic analysis also yields $T_{\text{eff}} = 5020 \pm 75 \text{ K}$ and $\log g = 3.52 \pm 0.08$. Interpolation of the star’s color, absolute magnitude and metallicity onto the Girardi et al. (2002) stellar model grids provides a stellar mass estimate of $M_* = 1.64 M_\odot$, and an age of 2.2 Gyr . Consistent with its post-main-sequence evolutionary status, HD 167042 is chromospherically inactive with $\log R'_{\text{HK}} = -5.34$, as measured from its CaII H&K emission relative to the stellar continuum. We also estimate a radius $R_* = 4.30 \pm 0.070 R_\odot$ and luminosity $L_* = 10.5 \pm 0.050 L_\odot$.

The *Hipparcos* catalog lists 115 photometric measurements of HD 167042 spanning 3.25 years. The star is photometrically stable over this time baseline, with an rms scatter 11.2 mmag , which is slightly higher than the median measurement uncertainty of 6 mmag . Since a periodogram analysis of the photometric measurements shows no significant power at periods ranging from 2 to 1200 days, we expect that the contribution to the star’s radial velocity variability from star spots and radial pulsation should be small. We follow Johnson et al.

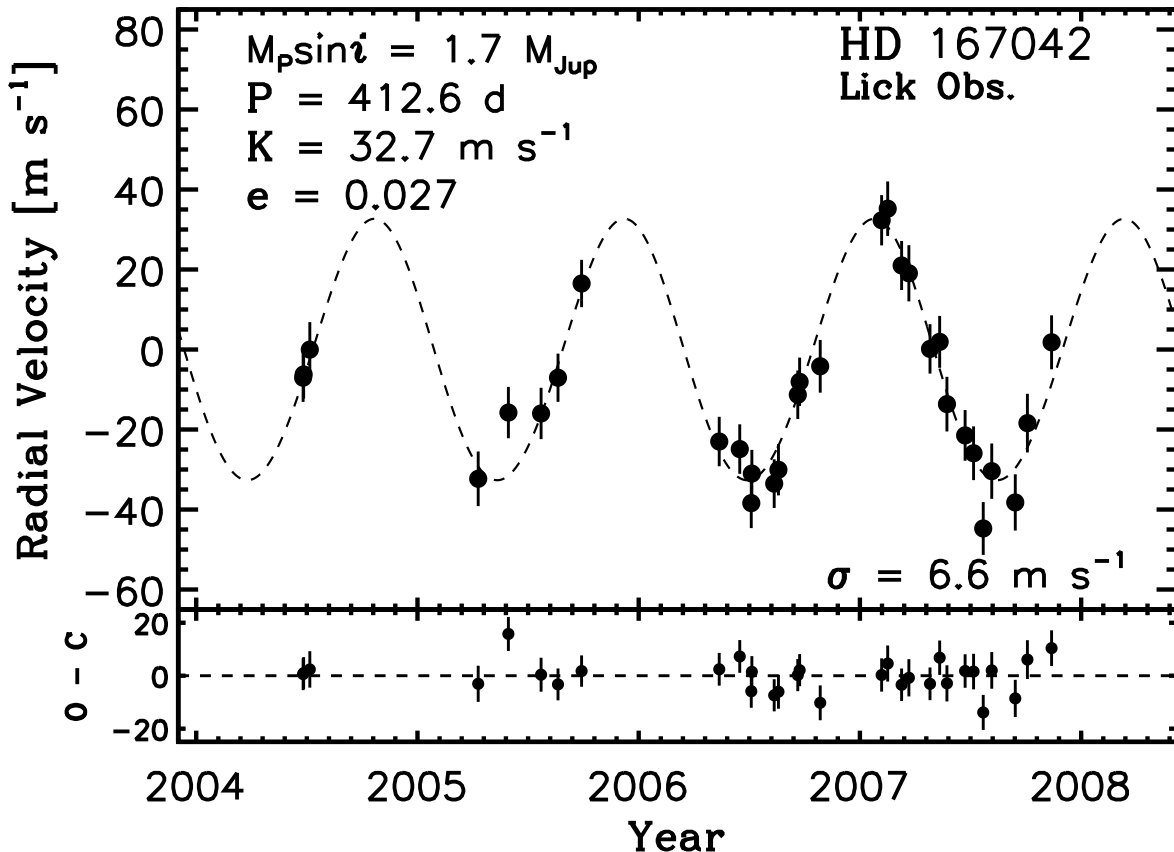


Fig. 3.— Radial velocity time series for HD 167042 measured at Lick Observatory. The dashed line shows the best-fit orbital solution, which has $\sqrt{\chi^2_\nu} = 1.01$.

(2007b) and adopt a jitter estimate of 5 m s^{-1} , based on the velocity scatter of other chromospherically quiet subgiants with properties similar to HD 167042.

We began monitoring HD 167042 in 2004 June and the first 10 observations, analyzed with a synthetic template, showed correlated variability with $\text{rms} = 15 \text{ m s}^{-1}$. We obtained a traditional, observed template to confirm the variations with higher Doppler precision. The full set of velocities is listed in Table 2 and plotted in Figure 3. The error bars in Figure 3 have been augmented by adding 5 m s^{-1} of jitter in quadrature to the internal measurement uncertainties.

The best-fit Keplerian orbital solution is shown in Figure 3. The solution has a 412.6 ± 4 day period, a semiamplitude $K = 32.7 \pm 2 \text{ m s}^{-1}$, and an eccentricity consistent with circular, $e = 0.027 \pm 0.04$. The residuals to the fit have $\text{rms} = 6.6 \text{ m s}^{-1}$ and reduced $\sqrt{\chi^2_\nu} = 1.01$, indicating that the scatter is adequately modeled by the internal measurement

uncertainties and estimated jitter. Assuming a stellar mass $M_* = 1.64 M_\odot$, the best-fit solution yields a semimajor axis $a = 1.3$ AU, and minimum planet mass $M_P \sin i = 1.7 M_{\text{Jup}}$. The orbital parameters are summarized in Table 4.

4. Summary and Discussion

We report the detection of two Jovian planets orbiting intermediate-mass subgiants. These detections come from our sample of evolved stars that we are monitoring at Lick and Keck Observatories. HD 167042 and κ CrB have masses significantly larger than solar, with $M_* = 1.64 M_\odot$ and $1.80 M_\odot$, respectively. Examination of the stars’ theoretical mass tracks reveals that these current-day subgiants began life on the main sequence as A-type dwarfs (Figure 1).

The relatively low-amplitude Doppler variations induced by κ CrBb and HD 167042b would not have been detectable if the stars were not in their current evolved state. Younger A- and F-type dwarfs have large rotational velocities ($V_{\text{rot}} \sin i \gtrsim 50 \text{ km s}^{-1}$) and excessive pulsation-induced velocity jitter that can mask the reflex velocity signal caused by a planet-mass companion (Galland et al. 2005). On the other hand, older stars ascending the red giant branch exhibit stochastic velocity variations in excess of 20 m s^{-1} (Hekker et al. 2006), which would make the planet orbiting κ CrB particularly difficult to detect since it induces a velocity amplitude of only 24.0 m s^{-1} . Subgiants, with their low rotation rates ($V_{\text{rot}} \sin i \lesssim 10 \text{ km s}^{-1}$) and low jitter ($< 10 \text{ m s}^{-1}$), occupy an observational “sweet spot” in the H–R diagram allowing our Doppler survey to probe to relatively low planetary masses in a wide range of orbital configurations.

The growing sample of planets around intermediate-mass stars is beginning to reveal important relationships between stellar mass and the properties of exoplanets. Of the 15 planets detected around evolved A-type stars ($M_* > 1.5 M_\odot$), none have been found orbiting closer than ~ 0.8 AU, with the majority orbiting at or beyond 1 AU (Johnson et al. 2007b). κ CrBb and HD 167042b are no exception to this trend, with semimajor axes of 2.7 AU and 1.3 AU, respectively. As noted by Johnson et al. (2007b), this cannot be due to a decrease in detection sensitivity since, for a given planet and stellar mass, the amplitude of the induced Doppler wobble scales as $a^{-1/2}$. Thus, the observed semimajor axis distribution of planets around A stars is significantly different from that of planets around lower-mass stars.

Johnson et al. (2007b) considered the possibility that the lack of close-in planets around K giants and clump giants may be attributable to engulfment by the expanding atmospheres of the central stars. However, stars crossing the subgiant branch do not undergo significant

expansion, with radii smaller than $\sim 5 R_{\odot}$ even at the base of the red giant branch. The fact that none of the 7 planets detected around massive subgiants ($M_* > 1.5 M_{\odot}$) has $a < 0.9$ AU strongly suggests that the lack of close-in planets around A stars is due to the effects of stellar mass on planet formation and migration, rather than post-main-sequence engulfment.

Stellar mass also plays an important role in the likelihood that a star harbors a detectable giant planet. By measuring the fraction of stars with planets in three widely spaced stellar mass bins, Johnson et al. (2007a) found that the occurrence rate of planets with $M_P \sin i > 0.8 M_{\text{Jup}}$ and $a < 2.5$ AU is a rising function of stellar mass. This analysis reveals that A stars appear to be planet-enriched by a factor of 4.5 compared to low-mass M dwarfs, with a measured giant planet occurrence rate of 9% for $1.3 < M_*/M_{\odot} \leq 1.9 M_{\odot}$. The planet fraction for higher-mass stars was based in part on three strong planet candidates from our survey of subgiants, one of which is announced here (HD 167042b; κ CrBb orbits beyond the 2.5 AU cut-off). This result indicates that stellar mass is a strong tracer of planeticity, which has important implications for the target selection of future planet searches. Just as stellar metallicity is exploited in the search for short-period planets around Sun-like stars (Fischer & Valenti 2005; Fischer et al. 2005; da Silva et al. 2006), stellar mass should be an important consideration in the selection of targets for future photometric, astrometric, and high-contrast direct imaging surveys.

The rising trend in planet occurrence toward higher stellar masses also informs models of planet formation. Several theoretical studies of the effects of stellar mass on planet formation have predicted that M stars should harbor fewer Jovian planets than Sun-like dwarfs (Laughlin et al. 2004; Ida & Lin 2005). More recently Kennedy & Kenyon (2007) studied planet formation at higher masses by accounting for the evolving disk mid-plane temperature due to stellar irradiation and viscous evolution. They predict that the fraction of stars with Jupiters should rise up to a peak of $\approx 20\%$ near $M_* = 3 M_{\odot}$.

Testing this prediction requires searching for planets around stars with masses greater than $2 M_{\odot}$. Unfortunately, the mass range of suitable subgiants is limited to $M_* \lesssim 2.2 M_{\odot}$, primarily due to our absolute magnitude criterion of $M_V > 2.0$ (see § 2). Doppler surveys of massive K giants with $M_* > 2.5 M_{\odot}$ provide perhaps the most favorable avenue for exploring the occurrence rate of planets around more massive A stars (Frink et al. 2001; Sato et al. 2005; Niedzielski et al. 2007). In particular, Lovis & Mayor (2007) are searching for planets around K giants in open clusters, which allows them to take advantage of the uniform ages of the cluster members to derive accurate stellar masses. The preliminary results from their survey indicate that stars more massive than $\sim 2 M_{\odot}$ have an enhanced abundance of super-Jupiters and brown dwarfs compared to lower-mass stars.

To enlarge the statistical ensemble of planets detected around intermediate-mass stars, we have expanded our planet search by adding 300 additional subgiants at Lick and Keck Observatories. If our current 9% detection rate holds, our expanded planet search is expected to yield an additional 20-30 planets over the next 3 years. Together with the detections from Doppler surveys of K giants and clump giants, the increased number of planets orbiting intermediate-mass stars will add significantly to our understanding of the effects of stellar mass on planet formation and planetary system architecture.

We extend our gratitude to the many CAT observers who have helped with this project, including Chris McCarthy, Raj Sareen, Howard Isaacson, Joshua Goldston, Bernie Walp, and Shannon Patel. We also gratefully acknowledge the efforts and dedication of the Lick Observatory staff, and the time assignment committee of the University of California for their generous allocations of observing time. JAJ is an NSF Astronomy and Astrophysics Postdoctoral Fellow and acknowledges support from the NSF grant AST-0702821. We appreciate funding from NASA grant NNG05GK92G (to GWM). DAF is a Cottrell Science Scholar of Research Corporation and acknowledges support from NASA Grant NNG05G164G that made this work possible. PKGW is supported by an NSF Graduate Research Fellowship. This research has made use of the SIMBAD database operated at CDS, Strasbourg France, and the NASA ADS database.

REFERENCES

- Bonfils, X., Forveille, T., Delfosse, X., Udry, S., Mayor, M., Perrier, C., Bouchy, F., Pepe, F., Queloz, D., & Bertaux, J.-L. 2005, *A&A*, 443, L15
- Butler, R. P., Johnson, J. A., Marcy, G. W., Wright, J. T., Vogt, S. S., & Fischer, D. A. 2006a, *PASP*, 118, 1685
- Butler, R. P., Marcy, G. W., Williams, E., McCarthy, C., Dosanjuh, P., & Vogt, S. S. 1996, *PASP*, 108, 500
- Butler, R. P., Wright, J. T., Marcy, G. W., Fischer, D. A., Vogt, S. S., Tinney, C. G., Jones, H. R. A., Carter, B. D., Johnson, J. A., McCarthy, C., & Penny, A. J. 2006b, *ApJ*, 646, 505
- da Silva, R., Udry, S., Bouchy, F., Mayor, M., Moutou, C., Pont, F., Queloz, D., Santos, N. C., Ségransan, D., & Zucker, S. 2006, *A&A*, 446, 717
- Endl, M., Cochran, W. D., Kürster, M., Paulson, D. B., Wittenmyer, R. A., MacQueen, P. J., & Tull, R. G. 2006, *ApJ*, 649, 436
- ESA, . 1997, *VizieR Online Data Catalog*, 1239, 0
- Fischer, D. A., Laughlin, G., Butler, P., Marcy, G., Johnson, J., Henry, G., Valenti, J., Vogt, S., Ammons, M., Robinson, S., Spear, G., Strader, J., Driscoll, P., Fuller, A., Johnson, T., Manrao, E., McCarthy, C., Muñoz, M., Tah, K. L., Wright, J., Ida, S., Sato, B., Toyota, E., & Minniti, D. 2005, *ApJ*, 620, 481
- Fischer, D. A. & Valenti, J. 2005, *ApJ*, 622, 1102
- Flower, P. J. 1996, *ApJ*, 469, 355
- Frink, S., Quirrenbach, A., Fischer, D., Röser, S., & Schilbach, E. 2001, *PASP*, 113, 173
- Galland, F., Lagrange, A.-M., Udry, S., Chelli, A., Pepe, F., Queloz, D., Beuzit, J.-L., & Mayor, M. 2005, *A&A*, 443, 337
- Girardi, L., Bertelli, G., Bressan, A., Chiosi, C., Groenewegen, M. A. T., Marigo, P., Salasnich, B., & Weiss, A. 2002, *A&A*, 391, 195
- Hekker, S., Reffert, S., Quirrenbach, A., Mitchell, D. S., Fischer, D. A., Marcy, G. W., & Butler, R. P. 2006, *A&A*, 454, 943
- Ida, S. & Lin, D. N. C. 2005, *ApJ*, 626, 1045

- Johnson, J. A., Butler, R. P., Marcy, G. W., Fischer, D. A., Vogt, S. S., Wright, J. T., & Peek, K. M. G. 2007a, ArXiv e-prints, 707
- Johnson, J. A., Fischer, D. A., Marcy, G. W., Wright, J. T., Driscoll, P., Butler, R. P., Hekker, S., Reffert, S., & Vogt, S. S. 2007b, ApJ, 665, 785
- Johnson, J. A., Marcy, G. W., Fischer, D. A., Henry, G. W., Wright, J. T., Isaacson, H., & McCarthy, C. 2006a, ApJ, 652, 1724
- Johnson, J. A., Marcy, G. W., Fischer, D. A., Laughlin, G., Butler, R. P., Henry, G. W., Valenti, J. A., Ford, E. B., Vogt, S. S., & Wright, J. T. 2006b, ApJ, 647, 600
- Kennedy, G. M. & Kenyon, S. J. 2007, ArXiv e-prints, 710
- Laughlin, G., Bodenheimer, P., & Adams, F. C. 2004, ApJ, 612, L73
- Lovis, C. & Mayor, M. 2007, A&A, 472, 657
- Marcy, G. W. & Butler, R. P. 1992, PASP, 104, 270
- Niedzielski, A., Konacki, M., Wolszczan, A., Nowak, G., Maciejewski, G., Gelino, R. C., Shao, M., Shetrone, M., & Ramsey, L. W. 2007, ArXiv e-prints, 705
- Reffert, S., Quirrenbach, A., Mitchell, D. S., Albrecht, S., Hekker, S., Fischer, D. A., Marcy, G. W., & Butler, R. P. 2006, ApJ, 652, 661
- Sato, B., Izumiura, H., Toyota, E., Kambe, E., Takeda, Y., Masuda, S., Omiya, M., Murata, D., Itoh, Y., Ando, H., Yoshida, M., Ikoma, M., Kokubo, E., & Ida, S. 2007, ApJ, 661, 527
- Sato, B., Kambe, E., Takeda, Y., Izumiura, H., Masuda, S., & Ando, H. 2005, PASJ, 57, 97
- Takeda, G., Ford, E. B., Sills, A., Rasio, F. A., Fischer, D. A., & Valenti, J. A. 2007, ApJS, 168, 297
- Valenti, J. A. & Fischer, D. A. 2005, ApJS, 159, 141
- Vogt, S. S. 1987, PASP, 99, 1214
- Wright, J. T. 2005, PASP, 117, 657
- Wright, J. T., Marcy, G. W., Butler, R. P., & Vogt, S. S. 2004, ApJS, 152, 261

Wright, J. T., Marcy, G. W., Fischer, D. A., Butler, R. P., Vogt, S. S., Tinney, C. G., Jones, H. R. A., Carter, B. D., Johnson, J. A., McCarthy, C., & Apps, K. 2007, ApJ, 657, 533

Table 1. Radial Velocities for HD 142091

JD -2440000	RV (m s ⁻¹)	Uncertainty (m s ⁻¹)
13121.906	-24.17	3.84
13122.948	-24.82	3.99
13123.890	-24.02	4.06
13131.838	-21.67	3.73
13134.904	-26.75	3.79
13144.858	-15.39	4.29
13145.887	-15.79	4.11
13223.735	-14.37	3.69
13242.679	-9.87	3.75
13470.970	18.04	4.43
13476.824	16.88	3.83
13503.906	30.83	4.39
13518.921	13.77	3.90
13573.710	12.21	4.01
13575.763	27.63	4.27
13602.694	17.93	3.45
13640.657	28.65	2.89
13870.807	-3.93	3.79
13880.793	22.74	2.63
13884.772	11.16	2.88
13891.828	11.43	2.84
13894.805	-6.89	3.14
13896.825	-11.82	3.32
13898.750	8.43	3.20
13900.783	9.57	3.22
13901.780	16.00	3.76
13922.745	-2.59	3.44
13923.811	10.59	2.91
13924.765	6.76	3.32
13925.805	-0.57	3.43

Table 1—Continued

JD -2440000	RV (m s ⁻¹)	Uncertainty (m s ⁻¹)
13926.747	0.48	3.15
13951.678	-4.63	3.34
13998.623	5.82	3.94
14131.082	-13.79	4.50
14137.046	-16.25	3.84
14147.025	-14.85	4.71
14169.962	-26.75	3.66
14171.015	-27.46	4.17
14233.764	-21.38	4.84
14255.856	-44.28	3.50
14274.812	-25.60	3.89
14304.755	-23.46	4.35
14318.753	-13.02	4.92
14336.656	-24.74	3.62
14337.658	-26.46	2.43
14338.661	-15.85	3.03

Table 2. Radial Velocities for HD 167042

JD -2440000	RV (m s ⁻¹)	Uncertainty (m s ⁻¹)
13181.937	5.64	3.40
13182.835	6.45	3.36
13192.971	12.66	4.71
13471.006	-19.63	4.64
13520.854	-3.08	4.03
13574.796	-3.30	4.02
13602.721	5.63	3.36
13641.710	29.19	3.16
13868.944	-10.32	3.64
13902.825	-12.20	3.64
13921.848	-25.72	3.73
13922.772	-18.33	3.18
13959.673	-20.84	3.46
13966.672	-17.38	4.00
13998.646	1.37	3.44
14001.669	4.61	3.42
14035.620	8.49	4.29
14137.078	44.99	3.81
14147.063	47.89	4.63
14170.039	33.69	3.56
14182.036	31.74	4.94
14216.930	12.83	3.63
14232.868	14.60	4.14
14244.873	-0.97	4.65
14274.859	-8.79	3.88
14288.829	-13.25	4.49
14304.764	-32.06	4.32
14318.828	-17.73	4.78
14357.668	-25.54	4.93
14377.725	-5.72	5.36

Table 2—Continued

JD	RV	Uncertainty
-2440000	(m s ⁻¹)	(m s ⁻¹)
14417.653	14.48	4.52

Table 3. Stellar Parameters

Parameter	κ CrB ^a	HD 167042
V	4.79	5.97
M_V	2.32	2.48
B-V	0.996	0.943
Distance (pc)	31.1	50.0
[Fe/H]	+0.14 (0.05)	+0.05 (0.06)
T_{eff} (K)	4960 (70)	5020 (75)
$V_{rot} \sin i$ (km s ⁻¹)	3.0 (0.5)	2.5 (0.5)
$\log g$	3.45 (0.09)	3.52 (0.08)
M_* (M_\odot)	1.80 (0.11)	1.64 (0.13)
R_* (R_\odot)	4.71 (0.08)	4.30 (0.07)
L_* (L_\odot)	12.3 (0.04)	10.5 (0.05)
Age (Gyr)	2.5 (1.0)	2.2 (1.0)
S_{HK}	0.10	0.11
$\log R'_{HK}$	-5.40	-5.34

^aHD 142091

Table 4. Orbital Parameters

Parameter	κ CrBb ^a	HD 167042b
P (d)	1208 (30)	412.6 (4)
T_p ^b (JD)	2453102 (100)	2453330 (130)
e	0.146 (0.08)	0.027 (0.04)
K (m s ⁻¹)	24.0 (1)	32.7 (2)
ω (deg)	204 (30)	29 (50)
$M_P \sin i$ (M_{Jup})	1.8	1.7
a (AU)	2.7	1.3
Fit RMS (m s ⁻¹)	6.0	6.6
Jitter (m s ⁻¹)	5.0	5.0
$\sqrt{\chi_\nu^2}$	0.97	1.01
N_{obs}	48	31

^aHD 142091 b

^bTime of periastron passage.